Original Article

JER

https://doi.org/10.12965/jer.2550086.043

Journal of Exercise Rehabilitation 2025;21(2):79-91

Effects of neuromuscular electrical stimulation on neuromuscular function and muscle quality in patient following anterior cruciate ligament reconstruction

Hyeon-Deok Jo[1], Maeng-Kyu Kim[1,2,*]

[1]Sports Science Research Institute, Kyungpook National University, Daegu, Korea
[2]Sports Medicine Lab, Department of Physical Education, Kyungpook National University, Daegu, Korea

Anterior cruciate ligament reconstruction (ACLR) leads to quadriceps neuromuscular dysfunction, including impaired force control and muscle degradation. Neuromuscular electrical stimulation (NMES) is widely used in rehabilitation to improve muscle mass and strength; however, its effects on neuromuscular functions and muscle quality, such as motor unit (MU) behavior and force steadiness (FS), remain unclear. This study investigated the effects of NMES on neuromuscular function and muscle quality in individuals with ACLR who could walk normally. Ten male ACLR patients underwent NMES 3 times weekly for 6 weeks, with 30 contractions per session. Neuromuscular function was assessed via FS, maximum voluntary isometric contraction (MVIC), and MU behavior in the rectus femoris and vastus lateralis. Muscle quality was evaluated using muscle thickness (MT), echo intensity (EI), and ultrasound texture features. Measurements were taken at baseline and weeks 3 and 6. NMES significantly improved MVIC, FS, MU behavior, and muscle quality (MT, EI, and homogeneity) on the ACLR side, with significant interaction effects observed. At week 3, MVIC and FS showed no significant improvement; however, structural and qualitative muscle changes were evident. NMES effectively enhanced neuromuscular function, MU behavior, and muscle quality impaired by ACLR. However, a 3-week intervention may not be sufficient for optimal neuromuscular recovery, highlighting the need for extended NMES protocols.

Keywords: Anterior cruciate ligament, Neuromuscular electrical stimulation, Neuromuscular function, Motor unit behavior, Muscle quality

INTRODUCTION

Anterior cruciate ligament (ACL) ruptures are a common sports injury. Hence, subsequent ACL reconstruction (ACLR) is conducted to prevent any ensuing arthritis and restore normal function (Davies et al., 2017; Mall et al., 2014). After ACLR, the unloading and immobilization of the knee joint inevitably result in muscle atrophy of the quadriceps, potentially leading to increased intramuscular fatty infiltration and quadricep neuromuscular degradation, such as decreased muscle strength, defined as arthrogenic muscle inhibition (AMI) (Lepley et al., 2020; Rice and McNair, 2010). The incidences of AMI are significantly higher in the first few months after surgery and tend to decrease gradually during rehabilitation, yet can also persist for many years (Ingersoll et al., 2008). For instance, less than 20% of elite football players who completed a rehabilitation protocol were reported to achieve a limb symmetry criterion of ≥90% in the strength tests (Herrington et al., 2021). Persistent AMI can lead to the early onset of osteoarthritis (Palmieri-Smith and Lepley, 2015; Palmieri-Smith et al., 2008) and an increased risk of a second ACL injury (Kyritsis et al., 2016). Although the mechanisms through which AMI onset occurs are not fully understood, some studies have reported that weakness in the peripheral nervous system, such as threshold inhibition of Ia afferent fibers and low gamma and alpha motor neuron recruitment, may contribute to knee extensor strength deficits (Johnson and Heckman, 2014; Konishi et al., 2002). Furthermore, decreased spinal reflex excitability after ACLR, which may contribute to pain, edema, and weakness of the mechanoreceptor respon-

*Corresponding author: Maeng-Kyu Kim https://orcid.org/0000-0002-7855-608X
Department of Physical Education, Kyungpook National University, 80 Daehak-ro, Buk-gu, Daegu 41566, Korea
Email: kimmk@knu.ac.kr
Received: February 2, 2025 / Revised: February 12, 2025 / Accepted: February 20, 2025

sible for neuromuscular control (Krogsgaard et al., 2011; Rice and McNair, 2010), may also induce altered knee force variability during submaximal isometric contraction tasks (Skurvydas et al., 2011).

The neuromuscular function is expressed as the ability to generate and regulate muscle force; force steadiness (FS) is the ability to maintain target force during submaximal contractions, quantified by the coefficient of variation (CV) of force variability. Meanwhile, an increased CV of force is associated with muscle stability, suggesting a diminished control in force variability (Enoka and Farina, 2021; Jo and Kim, 2023). Furthermore, although motor unit (MU) behaviors, including the MU action potential (MUAP), firing rate (FR), and MU number, contribute significantly to force production and muscle activation (Farina et al., 2016), the impact of ACLR on MU behaviors has yet to be elucidated. Additionally, the changes in the MU properties during submaximal contractions over an extended period are inconsistent, with some studies reporting a progressive increase in FR. This increase has been attributed to neural properties that regulate the recruited MU to maintain the target force (Kuchinad et al., 2004; Mettler and Griffin, 2016).

Furthermore, the qualitative and structural characteristics of muscles play a major role in neuromuscular functions. The echo intensity (EI) measures the degree of ultrasound echo caused by differences in tissue density within the muscle, thereby reflecting the muscle quality. Thus, an increase in EI can be attributed to adipose tissue infiltration due to prolonged periods of immobility or the infiltration of blood and fluid due to injury, which is associated with reduced muscle quality and a decline in strength output (Pillen et al., 2009). Moreover, the gray level co-occurrence matrix (GLCM) texture analysis and high-dimensional ultrasound analysis can complement EI, which does not account for the grayscale distribution in the image. This allows muscle quality to be assessed based on the relationship between neighboring pixels within a region of interest (ROI) (Sahinis and Kellis, 2023). A recent study found a significant association between the GLCM texture properties of the hamstring muscle and maximal flexion strength using texture analysis. This relationship was attributed to the differences in intramuscular biomaterial properties induced by intramuscular infiltration of fat or connective tissues (Sahinis and Kellis, 2023). It has also been reported that texture features can be used to assess subtle changes (muscle damage) that EI cannot evaluate (Jo and Kim, 2024). In other words, assessing the structural and qualitative properties of muscles, including muscle texture features, can provide new information in assessing neuromuscular control and joint functions.

Various techniques have been employed to improve neuromuscular functions (Koyama et al., 2010; Marmon et al., 2011), with neuromuscular electrical stimulation (NMES) being recognized as an effective method for enhancing neuromuscular function and muscle structural properties (Bezerra et al., 2011). The use of NMES in the early rehabilitation phase after ACLR has been shown to have a positive effect on the recovery of neuromuscular functions (Hasegawa et al., 2011). Specifically, the authors reported that early NMES application after ACLR was able to reduce muscle thickness loss and improve muscle strength decline. However, the majority of studies have been limited to the effects of NMES on isolated muscle strength and structural properties (Hasegawa et al., 2011; Labanca et al., 2018), with a lack of research on the effects on neuromuscular system behavior and qualitative muscle properties. Therefore, the purpose of this study was to evaluate the effectiveness of NMES application after ACLR on neuromuscular function and muscle quality by evaluating FS and MU behaviors, as well as texture features derived from ultrasound images, including EI.

MATERIALS AND METHODS

Ethical approval

The requirements, benefits, potential risks, and inconveniences of the study were explained to the participants before the study. Written informed consent was obtained from all participants. The Institutional Review Board (IRB) of Kyungpook National University approved the study protocol (IRB No. 2023-0439). Strict adherence to the ethical guidelines of the Declaration of Helsinki (last modified in 2013) was maintained.

Participants

Before recruiting participants, a statistical power analysis was performed *a priori* estimation using G*Power (v 3.1.9.4, Kiel University, Kiel, Germany) to determine the sample size. The input parameters were as follows: statistical test = analysis of variance (ANOVA): repeated measures (RMs), within-between interaction; type I error rate of $\alpha = 0.05$; power $\beta = 0.8$; effect size $f = 0.3$; number of groups = 2 (ACLR leg vs. contralateral [CTL] leg); Number of measurements = 3; Corr among rep measures = 0.50; and Nonsphericity correction $\varepsilon = 1$. Therefore, the overall sample size was 20 (10 participants each have ACLR and contralateral leg). Participants were recruited via the university website's bulletin board and social media. The participants were male individuals aged at least 20 years who had undergone ACLR more than 4 months but less than 2 years before the study and could walk normally (Table 1).

 https://doi.org/10.12965/jer.2550086.043

The participants were limited to those who underwent their first ACLR, excluding those with previous knee injuries or other orthopedic surgery histories and cardiovascular disease. Ten participants who met the inclusion criteria signed an informed consent form after reviewing the study protocol approved by the Kyungpook National University IRB.

Experimental protocol

The participants visited the laboratory for a familiarization session at least 2 days before the main study to assess the baseline physical information and the structural and qualitative characteristics of their muscles at rest using ultrasound. Training and demonstration of submaximal isometric contraction for maximum voluntary isometric contraction (MVIC) assessment and FS at a knee joint angle of 90° were then performed on both the CTL and ACLR leg. On the day of the experiment, MVIC strength values were measured for the ACLR and CTL leg, and submaximal isometric contractions were performed at 70% of the MVIC values for FS assessment. Electromyography (EMG) and force data were recorded in real-time during MVIC and submaximal isometric contractions. Interventions were then performed on the ACLR quadriceps 3 times per week for 6 weeks, with the measured variables evaluated for CTL and ACL 24 hours after the last intervention at weeks 3 and 6, respectively (Fig. 1).

Table 1. Clinical characteristics of subjects (n = 10)

Variable	Value
Age (yr)	24.10 ± 1.36
Anthropometric	
Height (cm)	176.83 ± 1.34
Weight (kg)	78.03 ± 3.69
Body mass index (kg/m^2)	24.93 ± 1.07
Injury information	
Injured limb (right:left)	6:4
Time after ACLR (months)	10.60 ± 2.16
IKDC (score)	68.28 ± 6.30
Lysholm knee scoring scale	79.90 ± 4.64

Values are presented as mean ± standard error of the mean or number.
ACLR, anterior cruciate ligament reconstruction; IKDC, International Knee Documentation Committee Subjective Knee Evaluation Form.

NMES intervention

The intervention consisted of 30 contractions per session, conducted 3 times per week for 6 weeks (Lepley et al., 2015; Wellauer et al., 2022). NMES was applied to the unilateral quadriceps on the ACLR side, with the participants seated in a knee extension machine with the hip and knee joints fixed at 90°. The intervention was applied via four adhesive electrodes (5 × 5 cm) using a portable NMES device (Wireless Pro, Chattanooga, Guildford, UK). Each electrode was attached to the innervated surfaces of the vastus lateralis (VL) and vastus medialis and bilaterally to the innervated surface of the rectus femoris (RF) approximately 10 cm below the femoral triangle. The parameters were identical across the interventions: waveform or rectangular symmetrical pulses with a duration of 400 μsec, a stimulation period of 6.25:12.00 (on:off), an intensity of 50% MVIC, and a frequency of 100 Hz. During the stimulation, the participants were constantly reminded to relax their quadriceps fully (Maffiuletti, 2010; Nishikawa et al., 2021).

Force

A load cell with a built-in strain gauge (MNC-200L, CAS, Seoul, Korea) was used to measure the knee extension strength. The participants sat on a dynamometer (HumacNORM, CSMi, Stoughton, MA, USA) with a load cell attached and secured to the dynamom-

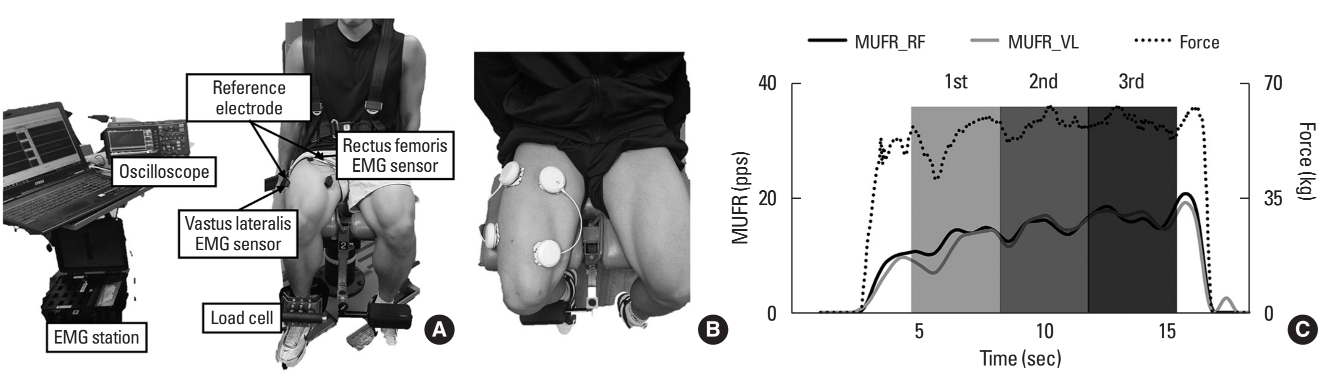

Fig. 1. Experimental procedure. (A, B) Experimental setup. (C) Motor unit behaviors and fore fluctuation during submaximal isometric contraction in three segments. EMG, electromyography; MUFR, motor unit firing rate; pps, pulse per second; RF, rectus femoris; VL, vastus lateralis.

eter with a belt to keep their upper body upright and limit pelvic movements. A strap was placed on the lateral malleolus of the ankle and connected to the load cell to record the muscle strength at a 90° knee angle. The analog signals were collected and digitized at 200 Hz with fourth-order Butterworth digital filtering using an oscilloscope (Infinii Vision 100 X, Keysight, Santa Rosa, CA, USA). The force data were analyzed using custom-made software.

To measure the MVIC strength, three maximal force efforts were performed, with a rest of 60 sec between the MVIC contractions. If any of the three MVIC strength values differed by >5% between two similar values, then an additional measurement was recorded. The highest MVIC strength values with a difference of 5% or less were selected for analysis and the submaximal isometric contraction session.

Isometric contractions were performed at 70% of the MVIC strength to assess FS. The participants were provided feedback to match and maintain the force exerted on the target level while seeing the target level displayed as a red line on a monitor 100 cm away from their eyes in real time. After practicing for 10 sec at the target force, the measurement consisted of two 15-sec contractions and a rest of 30 between the contractions. A custom-written MATLAB code (R2023b, MathWorks, Natick, MA, USA) was used to analyze the stable values in the data extracted during the submaximal isometric contractions and the 4-sec intervals. The most stable values were in the middle 8 sec of the 15-sec measurement, excluding the first 3.5 sec and the last 3.5 sec. The force data extracted during the submaximal isometric contractions were used to calculate CV as an indicator of FS.

Electromyography

To derive the characteristics of the neuromuscular system during MVIC and submaximal isometric contractions, signals were recorded for the RF and VL using a decomposition EMG sensor (Galileo, Delsys, Natick, MA, USA). The sensor attachment positions were set according to recommendations described by Zaheer et al. (2012). The skin was shaved and cleansed with alcohol before electrode attachment. The Nuprep gel was used to minimize skin electrical resistance, and sensors were attached to the muscle belly of each muscle along the direction of the muscle bundle. Inter-electrode impedance was measured using an impedance meter (EL-CHECK, BIOPAC Systems, Camino Goleta, CA, USA), kept below 2000 Ω.

Signals collected at 2000 Hz from each sensor were digitized and analyzed using a program dedicated to MU decomposition (Neuromap, Delsys, Natick, MA, USA). The 4-sec EMG signals were utilized for the analysis, where the same intervals with force data were selected and analyzed in the middle 8 sec, excluding the first 3.5 sec and the last 3.5 sec. MUAP, FR, and MU numbers were used in the study to evaluate the MU characteristics. To determine the differences in MU characteristics, the middle 9 sec was divided into three sections, excluding the first 3 sec and the last 3 sec, and all three sections were examined (Petrovic et al., 2022).

Ultrasound images

The B-mode images of the RF and VL were acquired using a 50-mm linear probe with 9.1–13 MHz mounted on an ultrasound machine (S12, SonoScape Co., Shenzhen, China). To acquire ultrasound images of the muscles at rest, the participants rested for 10 min in the supine position before measurement. Resting ultrasound images were acquired at the same locations as the surface EMG electrode attachments: transverse and longitudinal views of the RF and VL. Subsequently, the measurement sites were marked to ensure consistent image extraction. All images were acquired by a single examiner, in which the brightness, contrast, and focus of the ultrasound system were kept identical across all measurements. Three images of each muscle extracted at rest were stored on a computer, and the two images with the most similar EI were selected for analysis.

All acquired images were digitized at a resolution of 1,024×768 in the TIF format. The EI and GLCM features were determined using ImageJ (version 1.52a; National Institutes of Health, Bethesda, MD, USA) and a custom-made MATLAB Graphical User Interface (R2023b; MathWorks) based on identically sized (10×10 mm^2) ROI (6400-pixel ROIs = 80×80 pixels). The ROI was defined as the muscle region without the bone and septum that displayed the best reflection. The mean value of the grayscale histogram distribution (0–255 = black to white) was considered the EI. GLCM was derived from the angular relations between the neighboring pixels. The distance between them was defined as the number of pixel pair (i, j) occurrences for which the gray level i is away from the gray level j by a distance of d = 1 pixel, with orientation θ = average for 0°, 45°, 90°, and 135°. The following textural parameters were used (Jo and Kim, 2024; Matta et al., 2018).

$$\text{Entropy: } \sum_{i,j} p_{i,j}[-Ln(p_{i,j})]$$

$$\text{Energy: } \sum_{i,j=0}^{n-1}(p_{i,j})^2$$

$$\text{Homogeneity: } \sum_{i,j}\frac{p_{i,j}}{1+(i-j)^2}$$

Statistical analysis

All data are presented as the mean ± standard error and analyzed

https://doi.org/10.12965/jer.2550086.043

using IBM SPSS Statistics ver. 25.0 (IBM Co., Armonk, NY, USA). The normality for all parameters was analyzed using the Shapiro–Wilk test, which confirmed that the data followed a normal distribution. Levene test was applied to evaluate the homogeneity of variances. Since the normality assumption was satisfied, a paired t-test was used to compare CTL and ACL at each point and before and after each intervention. A one-way RMs ANOVA was used to compare the changes after the intervention with baseline measurements. A Bonferroni *post hoc* test was used to evaluate the differences with statistical significance. Two-way (time × side) RM-ANOVA was used to compare the effects of NMES between the bilateral legs. A Bonferroni *post hoc* test assessed the differences between the bilateral legs when interaction effects were significant. The significance level was set at $P < 0.05$.

RESULTS

Force

The differences within and between the bilateral legs in the MVIC showed that the ACL was significantly lower than the CTL before the intervention ($P < 0.01$). After the intervention, there was no difference between the bilateral legs ($P > 0.05$). In addition, there was no significant difference in CTL before and after the intervention. However, the intervention significantly increased the MVIC for the ACL compared to the baseline measurements ($P < 0.01$). A two-way RMs-ANOVA was performed for these changes; Mauchly's test indicated that the sphericity assumption was not violated (W = 0.757, χ^2 [2] = 4.729, $P > 0.05$). A significant interaction was observed between time and side (F [2, 36] = 5.820, $P < 0.01$, partial $\eta^2 = 0.244$), with a significant difference noted between the CTL (3.15% ± 2.47%) and ACL (19.91% ± 5.56%) at week 6 ($P < 0.01$). In addition, a one-way RMs-ANOVA was performed to determine the difference in the MVIC changes for the CTL and ACL over time, whereby the ACL changed significantly ($P < 0.01$), yet no significant difference was noted for the CTL ($P > 0.05$). The ACL significantly differed from the baseline measurements at week 6 ($P < 0.01$) (Figs. 2 and 3).

Furthermore, the differences within and between the bilateral legs in the FS revealed that the ACL was significantly higher than the CTL before the intervention ($P < 0.01$). After the intervention, there was no difference between the bilateral legs ($P > 0.05$). In addition, no significant difference was observed for the CTL before or after the intervention. The FS of the ACL was significantly decreased after the intervention compared to the baseline measurements ($P < 0.01$). A two-way RMs-ANOVA was conducted to determine the effect of FS on the interaction. Mauchly test indicated that the sphericity assumption was not violated (W = 0.735, χ^2 [2] = 5.239, $P > 0.05$). The results revealed a significant interaction effect between time and side (F [2, 36] = 5.547, $P < 0.01$, partial $\eta^2 = 0.236$), with significant differences between the bilateral legs at weeks 3 (CTL, 0.94% ± 0.25%; ACL, -0.85% ± 0.53%, $P < 0.01$) and 6 (CTL, -0.47% ± 0.45%; ACL, -2.14% ± 0.68%, $P < 0.01$). In addition, a one-way RMs-ANOVA was performed to determine the changes in FS for each leg over time. The CTL showed no statistically significant differences, while the ACL showed a significant decrease ($P < 0.01$), particularly at week 6, compared

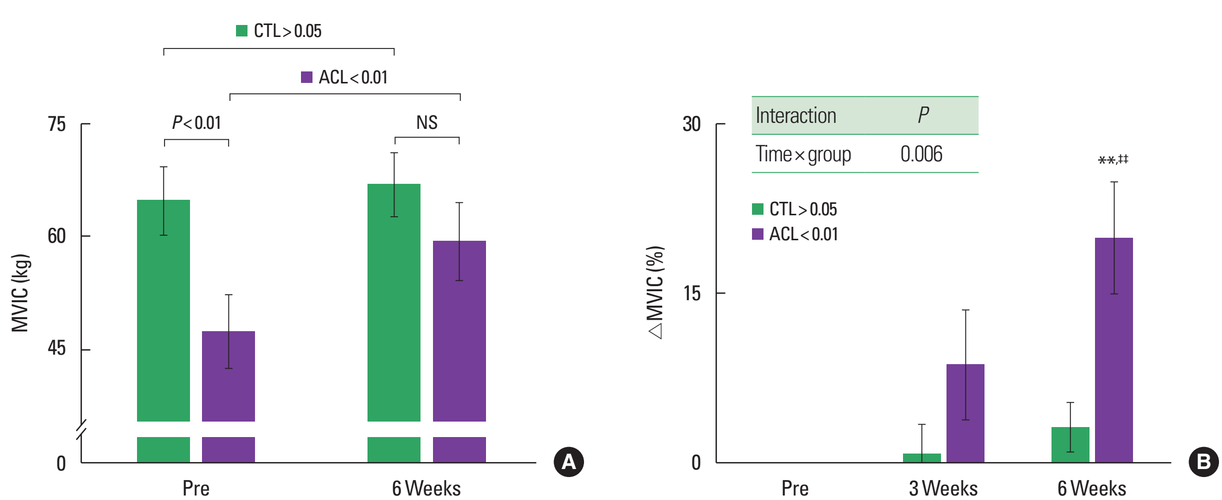

Fig. 2. Maximum voluntary isometric contraction (MVIC). (A) Differences in MVIC. (B) Changes in MVIC after intervention. ACL, anterior cruciate ligament; CTL, contralateral. **$P < 0.01$ indicates significant differences between the ACL and CTL at each time point, which were analyzed using the Bonferroni *post hoc* test. ‡‡$P < 0.01$ indicates significant differences in the ACL between the baseline and each time point, which were analyzed using the Bonferroni *post hoc* test.

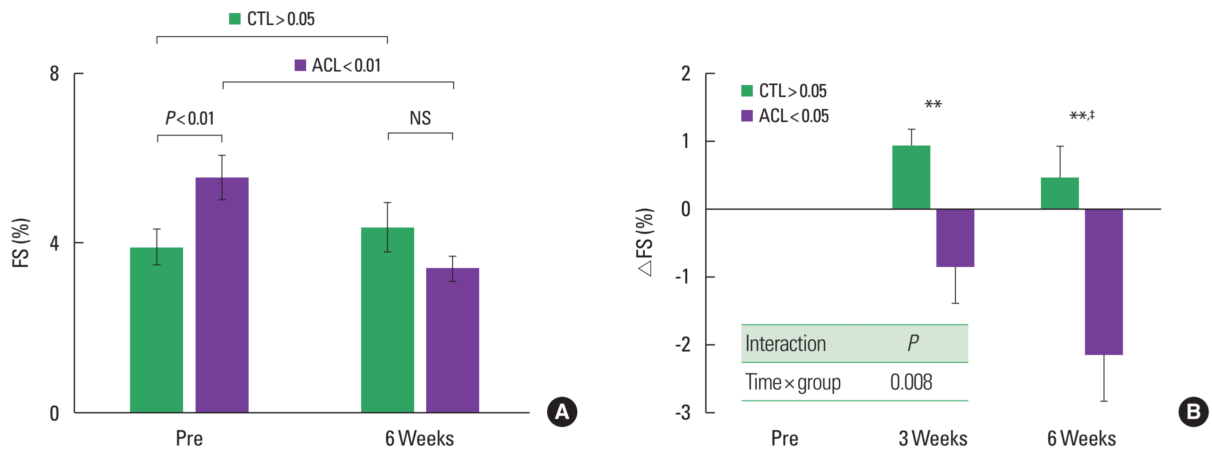

Fig. 3. Force steadiness (FS). (A) Difference in FS. (B) Changes in FS after intervention. ACL, anterior cruciate ligament; CTL, contralateral. $^{**}P<0.01$ indicates significant differences between the ACL and CTL at each time point, which were analyzed using the Bonferroni *post hoc* test. $^{‡}P<0.05$ indicates significant differences in the ACL between the baseline and each time point, which were analyzed using the Bonferroni *post hoc* test.

to the baseline measurements ($P<0.05$) (Figs. 2 and 3).

MU behaviors

The differences within and between the bilateral legs in the MU characteristics were also examined. Regarding MUAP, the RF of the ACL was significantly increased after the intervention compared to the baseline measurements ($P<0.05$). For FR, there were no significant differences within or between the groups. For the MU number, the VL of the ACL was significantly lower than for the CTL before the intervention ($P<0.05$), which significantly increased after the intervention compared to the baseline measurements ($P<0.01$). A two-way RMs-ANOVA was performed to determine the interaction effect between time and side of the MU characteristics. The MUAP, FR, and MU number showed no significant interaction effects for the RF and VL ($P>0.05$). Furthermore, a one-way RMs-ANOVA was performed to determine the changes in MU characteristics over time; the MUAP of the RF was significantly different for the ACL ($P<0.05$), specifically at week 3 (0.35% ± 0.09%), compared to the baseline measurements ($P<0.01$). Neither the RF nor VL exhibited significant differences in FR for either leg ($P>0.05$). For the MU number, the VL of the ACL was significantly different ($P<0.01$), specifically at week 6 (4.22 ± 0.93), compared to the baseline measurements ($P<0.01$) (Table 2).

Furthermore, results comparing the FR between segments during submaximal isometric contraction show the FR of the RF was significantly different for both the ACL and CTL before the intervention ($P<0.05$), with only the ACL showing a significant difference at week 3 ($P<0.05$). The FR of VL was significantly different for both the ACL ($P<0.01$) and CTL ($P<0.05$) before the intervention, with no significant difference after the intervention (Fig. 4).

Muscle structure and quality

The differences in the muscle structures within and between the bilateral legs showed that the MT in the RF and VL of the ACL significantly increased after the intervention compared to the baseline measurements ($P<0.01$). The RF was significantly different between the bilateral legs after the intervention ($P<0.05$), while the VL was significantly different between the bilateral legs before the intervention ($P<0.01$). A two-way RMs-ANOVA was performed to determine the interaction effect between time and the side of the muscle structures during the intervention. The MT of the RF did not violate the assumption of sphericity (W = 0.907, χ^2 [2] = 1.466, $P>0.05$). Based on the sphericity result, a significant interaction effect was noted between time and the muscle structure side (F [2, 32] = 22.184, $P<0.01$, partial $\eta^2=0.581$), with a significant difference between the CTL (0.845% ± 0.4174%) and ACL (15.633% ± 4.102%) at week 6 ($P<0.05$). As the MT of the VL violated Mauchly's sphericity assumption (W = 0.613, χ^2 [2] = 7.343, $P<0.05$), a Greenhouse–Geisser correction (ε = 0.721) was applied to examine the results. A significant interaction effect was identified between time and side (F [2, 23.07] = 12.029, $P<0.01$, partial $\eta^2=0.429$), with significant differences at week 3 (CTL, -0.33% ± 5.15%; ACL, 15.96% ± 3.53%; $P<0.05$) and week 6 (CTL, -1.38% ± 5.66%; ACL, 26.80% ± 2.83%; $P<0.01$). In addition, a one-way RMs-ANOVA was performed to determine the changes in muscle structure over time. While there were no significant differences in the VL for either group, the MT of the

 https://doi.org/10.12965/jer.2550086.043

Table 2. Changes in MU behaviors

Variable			Pre	6 Weeks	*P*-value	Δ 3 Weeks	Δ 6 Weeks	*P*-value	Interaction
MUAP × 10⁴ (mV)	RF	CTL	1.61 ± 0.42	1.41 ± 0.33	0.763	-0.11 ± 0.21	-0.20 ± 0.27	0.727	0.060
		ACL	1.28 ± 0.25	1.61 ± 0.34‡	0.024	0.35 ± 0.09‡‡	0.33 ± 0.26	0.028	
	VL	CTL	1.91 ± 0.26	1.67 ± 0.36	0.704	-0.11 ± 0.13	-0.24 ± 0.23	0.867	0.127
		ACL	1.70 ± 0.27	1.83 ± 0.31	0.103	0.29 ± 0.16	0.13 ± 0.35	0.100	
FR (pps)	RF	CTL	16.81 ± 0.75	13.45 ± 1.61	0.063	-1.60 ± 1.24	-3.36 ± 1.71	0.292	0.397
		ACL	15.92 ± 1.16	14.34 ± 2.02	0.890	0.30 ± 0.72	-1.58 ± 1.96	0.970	
	VL	CTL	17.73 ± 0.48	14.04 ± 1.74	0.068	-0.71 ± 0.72	-3.69 ± 2.06	0.115	0.058
		ACL	15.98 ± 0.78	14.77 ± 1.84	0.598	-1.40 ± 1.05	-1.20 ± 2.16	0.151	
MU number (count)	RF	CTL	13.10 ± 1.04	13.11 ± 0.90	1.000	-0.20 ± 1.65	0 ± 1.14	0.985	0.823
		ACL	13.20 ± 1.32	12.33 ± 1.66	0.382	-0.80 ± 1.34	-1.00 ± 1.02	0.655	
	VL	CTL	13.90 ± 1.23*	14.67 ± 1.07	0.375	3.10 ± 1.49	1.44 ± 1.46	0.043	0.109
		ACL	12.30 ± 1.10	15.78 ± 1.09‡‡	0.004	1.70 ± 1.30	4.22 ± 0.93‡‡	0.026	

Values are presented as mean ± standard error of the mean.
MU, motor unit; MUAP, motor unit action potential; RF, rectus femoris; VL, vastus lateralis; CTL, contralateral; ACL, anterior cruciate ligament reconstructed side; FR, firing rate.
P-values are calculated by one-way repeated measures analysis of variance (RM-ANOVA). Interaction values are calculated by two-way RM-ANOVA.
**P* < 0.05 indicate significant differences between the CTL and ACL at each time point, which were analyzed using the Bonferroni *post hoc* test. ‡*P* < 0.05, ‡‡*P* < 0.01 indicate significant differences in the ACL between baseline and each time point, which were analyzed using the Bonferroni *post hoc* test.

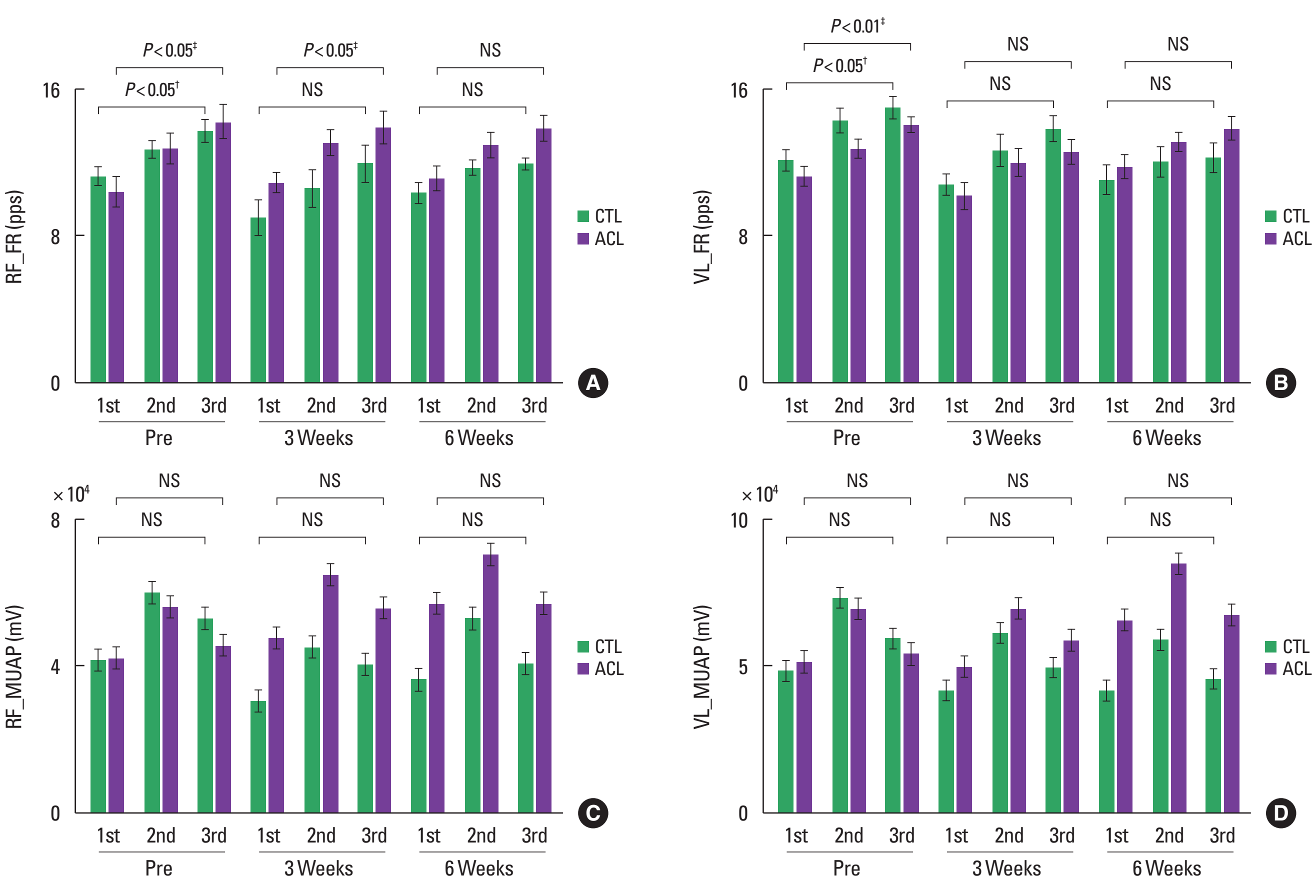

Fig. 4. FR and MUAP. (A, B) Differences in FR between segments. (C, D) Differences in MUAP between segments. RF, rectus femoris; VL, vastus lateralis; FR, firing rate; MUAP, motor unit action potential; ACL, anterior cruciate ligament; CTL, contralateral; ANOVA, analysis of variance; NS, not significant. †*P* indicates significant differences among the ACL at each time point, which were analyzed using ANOVA. ‡*P* indicates significant differences among the CTL at each time point, which were analyzed using ANOVA.

Table 3. Changes in muscle structure and quality

Variable			Pre	6 Weeks	*P*-value	Δ 3 Weeks	Δ 6 Weeks	*P*-value	Interaction
Muscle structure									
MT (cm)	RF	CTL	2.45 ± 0.11	2.44 ± 0.12*	0.580	2.3 ± 1.52	0.85 ± 1.32*	0.306	0.000
		ACL	2.38 ± 0.09	2.74 ± 0.11‡‡	0.000	8.43 ± 2.05‡	15.63 ± 1.30‡‡	0.000	
	VL	CTL	2.48 ± 0.13**	2.36 ± 0.13	0.639	-0.33 ± 5.15*	-1.38 ± 5.66**	0.883	0.001
		ACL	1.93 ± 0.16	2.3 ± 0.13‡‡	0.000	15.96 ± 3.53‡‡	26.8 ± 2.83‡‡	0.000	
Texture features									
Energy (a.u.)	RF	CTL	25.83 ± 2.92	24.3 ± 2.02**	0.422	-0.03 ± 0	-0.05 ± 0.07	0.468	0.001
		ACL	21.53 ± 2.36	33.12 ± 3.24‡‡	0.003	0.25 ± 0.00‡‡	0.37 ± 0.06‡‡	0.000	
	VL	CTL	20.61 ± 3.03	23.06 ± 3.31	0.132	-0.03 ± 0.09	0.11 ± 0.06	0.379	0.080
		ACL	12.98 ± 1.8	18.66 ± 2.62‡	0.020	0.23 ± 0.07‡	0.29 ± 0.08‡	0.001	
Correlation (a.u.)	RF	CTL	0.949 ± 0.007	0.938 ± 0.006	0.144	-0.32 ± 0.99	-1.11 ± 0.64	0.465	0.010
		ACL	0.956 ± 0.003	0.945 ± 0.005‡‡	0.004	-0.86 ± 0.37	-1.28 ± 0.34‡	0.014	
	VL	CTL	0.934 ± 0.006	0.939 ± 0.004	0.761	-0.15 ± 0.62	0.45 ± 0.43	0.866	0.555
		ACL	0.927 ± 0.005	0.931 ± 0.007	0.835	0.79 ± 0.54	0.38 ± 0.93	0.603	
Entropy (a.u.)	RF	CTL	9.69 ± 0.14	9.73 ± 0.14	0.515	0.08 ± 0.84	0.45 ± 0.75	0.568	0.001
		ACL	10.04 ± 0.17	9.41 ± 0.16‡‡	0.003	-4.83 ± 0.91‡‡	-8.06 ± 1.73‡	0.003	
	VL	CTL	10.01 ± 0.17	9.88 ± 0.2	0.203	-0.06 ± 0.94	-1.69 ± 1.05	0.331	0.432
		ACL	10.47 ± 0.16	10.04 ± 0.20‡	0.035	-3.65 ± 1.27	-5.62 ± 1.91	0.032	

Values are presented as mean ± standard error of the mean.
MT, muscle thickness; RF, rectus femoris; VL, vastus lateralis; CTL, contralateral; ACL, anterior cruciate ligament reconstructed side.
P-values are calculated by one-way repeated measures analysis of variance (RM ANOVA). Interaction values are calculated by two-way RM ANOVA.
**P* < 0.05, ***P* < 0.01 indicate significant differences between the CTL and ACL at each time point, which were analyzed using the Bonferroni *post hoc* test. ‡*P* < 0.05, ‡‡*P* < 0.01 indicate significant differences in the ACL between baseline and each time point, which were analyzed using the Bonferroni *post hoc* test.

RF and VL of the ACL were significantly different ($P < 0.01$). Specifically, the RF was significantly different from baseline at week 3 ($P < 0.05$) and week 6 ($P < 0.01$). The VL was also significantly different from baseline at weeks 3 and 6 ($P < 0.01$) (Table 3, Figs. 5 and 6).

Furthermore, the differences in muscle quality within and between the bilateral legs were examined. The EI in the RF and VL of the ACL were all significantly increased after the intervention compared to baseline ($P < 0.01$), with the RF being significantly different between the bilateral legs after the intervention ($P < 0.05$) and the VL being significantly different between the bilateral legs before the intervention ($P < 0.01$). For energy, the RF ($P < 0.01$) and VL ($P < 0.05$) of the ACL were both significantly different after the intervention compared to the baseline measurements, with the RF differing significantly between the bilateral legs after the intervention ($P < 0.01$). Comparatively, significant differences were observed for the VL between the bilateral legs before the intervention ($P < 0.05$). For correlation, the RF of the ACL was significantly different after the intervention compared to the baseline measurements ($P < 0.01$). For homogeneity, the RF and VL of the ACL significantly increased after the intervention compared to the baseline measurements ($P < 0.05$). The RF and VL significantly differed between the bilateral legs before the intervention ($P < 0.05$). For entropy, the RF of the ACL was significantly different after the intervention compared to the baseline measurements ($P < 0.01$), and the RF was significantly different between the bilateral legs after the intervention ($P < 0.05$). A two-way RMs-ANOVA was performed to determine the interaction effect for muscle quality between time and the structure side during the intervention period. The RF and VL did not violate Mauchly's sphericity assumption for EI (RF: $W = 0.875$, χ^2 [2] = 1.871, $P > 0.05$; VL: $W = 0.698$, χ^2 [2] = 5.387, $P > 0.05$). The sphericity results showed a significant interaction effect between time and side (RF: F [2, 32] = 9.626, $P < 0.01$, partial $\eta^2 = 0.391$; VL: F [2, 32] = 8.160, $P < 0.01$, partial $\eta^2 = 0.338$), for the RF at week 6 (CTL, -4.05% ± 1.67%; ACL, -20.52% ± 3.23%; $P < 0.01$), and the VL at week 3 (CTL, 0.34% ± 2.56%; ACL, -11.88% ± 3.64%; $P < 0.05$) and week 6 (CTL, -1.43% ± 2.36%; ACL, -16.98% ± 3.45%; $P < 0.01$). For the texture characteristics, the VL did not show a significant interaction effect; however, the energy and homogeneity data for the RF did not violate Mauchly's sphericity assumption (energy: $W = 0.870$, χ^2 [2] = 2.081, $P > 0.05$; homogeneity: $W = 0.811$, χ^2 [2] = 3.134, $P > 0.05$). Based on these sphericity results, there was a significant interaction effect between time and side (energy: F [2, 32] = 10.214,

 https://doi.org/10.12965/jer.2550086.043

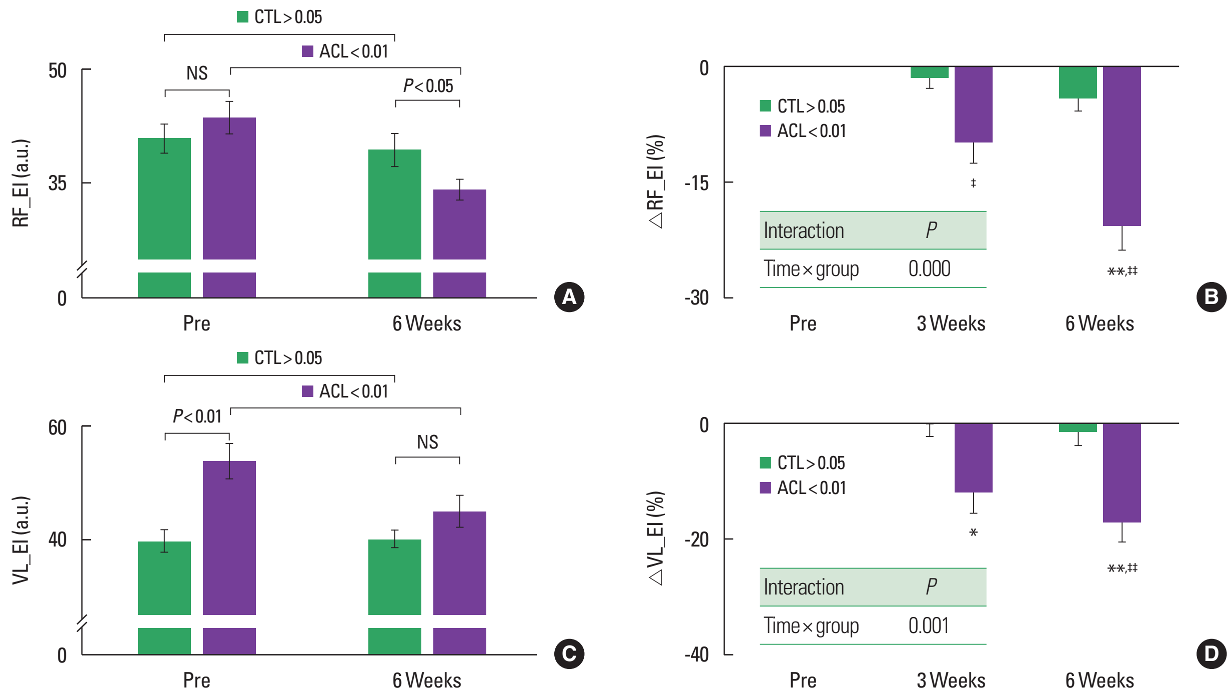

Fig. 5. Echo intensity (EI). (A, C) Differences in EI. (B, D) Changes in EI after intervention. RF, rectus femoris; VL, vastus lateralis; EI, echo intensity; ACL, anterior cruciate ligament; CTL, contralateral. *P < 0.05, **P < 0.01 indicate significant differences between the ACL and CTL at each time point, which were analyzed using the Bonferroni *post hoc* test. ‡P < 0.05, ‡‡P < 0.01 indicate significant differences in the ACL between the baseline and each time point, which were analyzed using the Bonferroni *post hoc* test.

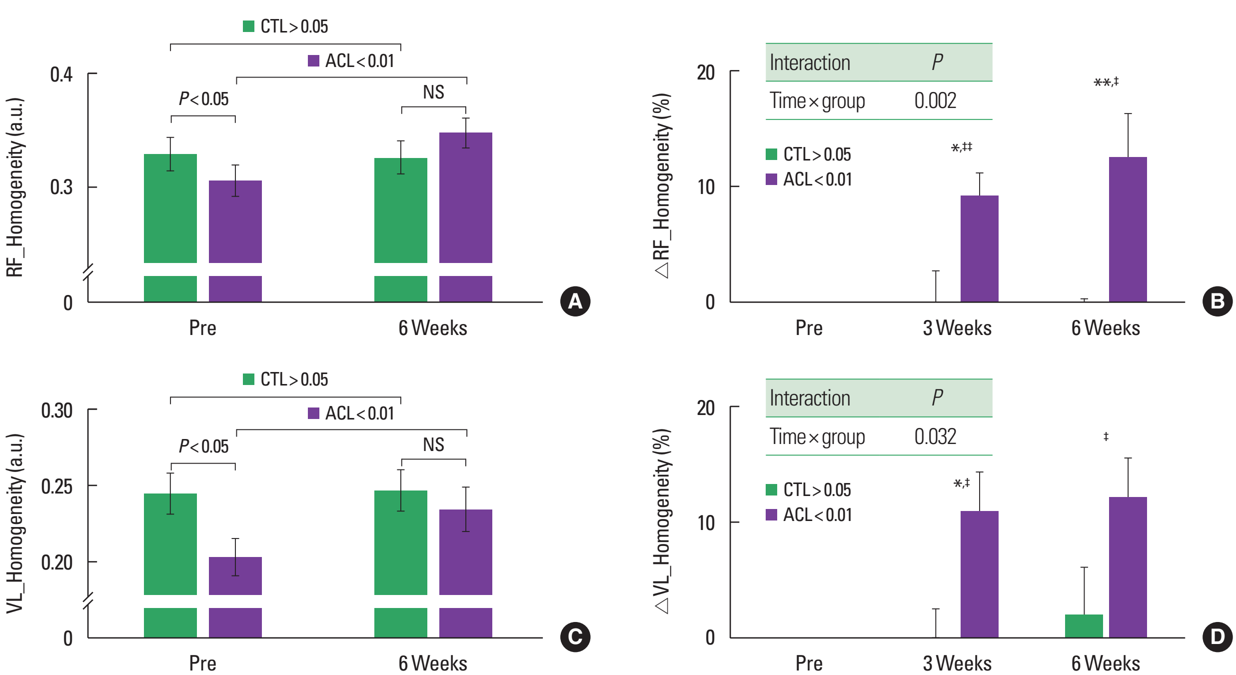

Fig. 6. Homogeneity. (A, C) Differences in homogeneity. (B, D) Changes in homogeneity after the intervention. RF, rectus femoris; VL, vastus lateralis ACL, anterior cruciate ligament; CTL, contralateral. *P < 0.05, **P < 0.01 indicate significant differences between the ACL and CTL at each time point, which were analyzed using the Bonferroni *post hoc* test. ‡P < 0.05, ‡‡P < 0.01 indicate significant differences in the ACL between the baseline and each time point, which were analyzed using the Bonferroni *post hoc* test.

$P<0.01$, partial $\eta^2=0.390$; homogeneity: F [2, 32] = 6.798, $P<0.01$, partial $\eta^2=0.298$). As entropy violated Mauchly's sphericity assumption (W = 0.647, χ^2 [2] = 6.526, $P<0.05$), the Greenhouse–Geisser correction was applied (ε = 0.739), revealing a significant interaction effect between time and side (F [2, 23.655] = 8.791, $P<0.01$, partial $\eta^2=0.355$). Specifically, energy was significantly lower at week 3 (CTL, 0.02% ± 0.07%; ACL, 0.25% ± 0.05%; $P<0.05$) and week 6 (CTL, -0.03 ± 0.06; ACL, 0.34 ± 0.06; $P<0.01$). Meanwhile, homogeneity was significantly lower at week 3 (CTL, -0.17% ± 2.82%; ACL, 9.14% ± 2.01%; $P<0.05$) and week 6 (CTL, -2.08% ± 2.39%; ACL, 12.47% ± 3.85%; $P<0.01$). Entropy showed significant differences between the bilateral legs at week 3 (CTL, -0.29% ± 0.80%; ACL, -4.65% ± 0.81%; $P<0.01$) and week 6 (CTL, 0.14% ± 0.65%; ACL, -6.80% ± 1.87%; $P<0.01$). Furthermore, a one-way RMs-ANOVA was performed to determine changes in muscle quality over time. While the EI of the CTL between the RF and VL did not differ significantly ($P>0.05$), the EI of the ACL showed statistically significant differences between the RF and VL ($P<0.01$). Specifically, the RF ($P<0.05$) at week 3 and the RF and VL at week 6 were significantly different compared to the baseline measurements ($P<0.05$). The energy, correlation, homogeneity, and entropy for the texture features significantly differed from the RF observed in the ACL ($P<0.05$). Specifically, the RF significantly differed from the baseline measurements in energy, homogeneity, and entropy at weeks 3 and 6 and the correlation at week 6 ($P<0.05$) (Table 3, Figs. 5 and 6).

DISCUSSION

The main findings of this study were as follows. First, there was a significant difference in MVIC between the bilateral legs before the intervention. After the intervention, MVIC in the ACL significantly increased compared to baseline measurements, indicating a significant interaction effect. Additionally, FS differed significantly between the bilateral legs before the intervention and was significantly reduced in the ACL after the intervention compared to baseline values, again showing a significant interaction. Second, in terms of MU characteristics, MUAP in the RF of the ACL significantly increased after the intervention. Furthermore, the number of MUs in the VL of the ACL also showed a significant increase compared to baseline measurements. Third, structural differences in the VL between the bilateral legs were observed before the intervention. A significant interaction effect was found in MT changes for both the RF and VL. Regarding muscle quality, the ACL showed significant improvement after the intervention, with a notable interaction effect between the bilateral legs, particularly in the RF.

After ACLR, the muscle strength became significantly lower on the contralateral side, described as a decrease in peripheral nervous system and spinal reflex excitability following injury and reconstruction (Lepley et al., 2020; Rice and McNair, 2010). In this study, MVIC significantly differed between the CTL and ACL before the intervention, which can be attributed to AMI following ACL injury and ACLR. Similarly, the mechanoreceptor loss in the ACL after the injury decreases feedback from gamma motor neurons and inhibits MU recruitment in the quadriceps. This reduces strength and FS during submaximal isometric contractions (Hollman et al., 2021; Spencer et al., 2020). The results of the present study also showed that the FS of the ACL before the intervention was significantly higher than that of the CTL, which aligns with previous studies. Various techniques have been used to improve poor musculoskeletal functions; NMES is particularly effective in achieving multiple positive outcomes. Specifically, Hasegawa et al. (2011) reported that early NMES application after ACLR can minimize muscle atrophy and decrease strength. Additionally, Labanca et al. (2018, 2022) reported that NMES application after ACLR significantly improves movement functions and strength (Labanca et al., 2022; Labanca et al., 2018). In the present study, 6 weeks of NMES intervention significantly increased the MVIC of the ACL, comparable to that of the CTL after the intervention. In addition, the FS of the ACL was significantly enhanced after the intervention. Therefore, similar to previous studies, NMES effectively improved neuromuscular functions, which ACLR decreased. Notably, there was no significant difference in the change at week 3; however, there was a significant difference at week 6, suggesting that 3 weeks of NMES is insufficient for strength recovery.

Regarding the changes in MU at the individual muscle level, the MUAP of the ACL showed a significant increase in the RF. Previous studies have reported a significant rise in MUAP and an increase in MVIC due to neural adaptations after resistance exercise training (Herda, 2022; Jenkins et al., 2021). Similarly, for the MU number, the VL of the ACL was also significantly increased following NMES, suggesting that these improvements in neuromuscular functions result from NMES-induced neural adaptations. Neuromuscular damage after ACLR can last several years, decreasing strength and muscle control, while inhibiting MU recruitment in the quadriceps (Hollman et al., 2021; Spencer et al., 2020). Meanwhile, the characteristics of the MUs reflect neuromuscular

https://doi.org/10.12965/jer.2550086.043

function. This study observed that the MUAP was relatively degraded in the RF, and the number of MUs was low in the VL. In other words, even in ACLR patients who can walk normally, their neuromuscular characteristics are still impaired; thus, NMES represents an effective method for improvement. Furthermore, the gradual increase in FR during sustained submaximal contraction was explained by the regulation of recruited MUs, i.e., force maintenance through increased FR (Herda, 2022). In the present study, the comparison of the sustained submaximal contraction duration gradually increased after being divided into three sections; moreover, each segment was significantly different from the other before the intervention. However, after the intervention, the significant differences between the groups disappeared, and only the RF of the ACL remained significant at week 3. This finding, whereby less variation was observed in the FR among MU characteristics while strength was sustained and FS improved, suggests that neuromuscular interventions can induce sufficient results with less exertion. However, in terms of simple comparison to preintervention, similar to the MVIC and FS results above, the lack of significant difference at week 3, while noting a significant difference at week 6, identical to the MVIC and FS results above, suggests that NMES should be applied for at least 6 weeks to improve neuromuscular function and its characteristics.

Various studies have used EI as an indicator of muscle quality to assess changes following muscle injury or exercise training (Ikezoe et al., 2020; Matta et al., 2018; Pillen et al., 2009). In the present study, the EI of the VL was significantly different between the bilateral legs due to baseline deterioration; however, no difference was noted after the intervention. The EI of the RF was not significantly different between the bilateral legs before the intervention but was significantly different after the intervention, with the RF improving better than the CTL. The RF and VL of the ACL were significantly reduced after the intervention, indicating improvements in muscle quality. However, the RF did not show a significant difference compared to the CTL at baseline, possibly due to different changes in each muscle within the quadriceps after the ACL injury. Indeed, muscle atrophy predominantly occurs in the quadriceps after ACL injury; however, only a relatively minor amount of atrophy was observed in the RF, with the most atrophy occurring in the VL or VI (Akima and Furukawa, 2005; Yang et al., 2019). Type I myofibers are the most sensitive to atrophy; indeed, the VL and VI muscles have a predominance of Type I myofibers (Lepley et al., 2020). Similarly, the MT of the RF was not significantly different from the CTL at baseline in this study; however, the VL was significantly different from the CTL, and both the RF and VL increased significantly after intervention, with the RF being significantly larger than the CTL. Meanwhile, the VL was restored and was no longer significantly different from the CTL. This improvement was seen for both EI and GLCM. Conversely, the EI of the RF did not significantly differ between bilateral legs before intervention, but homogeneity did. Furthermore, the VL showed no significant change at week 3, but again, homogeneity did. While only one-dimensional information is displayed for EI, based on the light and dark regions, the texture characteristics can provide more in-depth information when combined with the pixel relationship data. Indeed, GLCM texture features can be used to observe exercise-induced muscle damage (Jo and Kim, 2024; Matta et al., 2018). Moreover, our previous research has demonstrated that the GLCM characteristics can identify subtle damage or changes that EI cannot (Jo and Kim, 2024). Hence, the present study showed significant differences in muscle quality characteristics even in the RF and VL. Although the RF was not significantly different from the CTL before the intervention, it demonstrated improved quality characteristics after NMES intervention; meanwhile, the VL showed a significant effect at week 3 and recovered to be similar to the CTL at week 6. This suggests that 6 weeks of NMES rather than 3 weeks is required to improve the quality of the injured muscle, and the different levels of damage between individual muscles before treatment and the subtle changes in each muscle after intervention can be seen using the GLCM texture features.

This study has several limitations. Firstly, high frequencies were selected for NMES; this limits the results from being generalized to those obtained using other lower frequencies. However, frequencies above 50 Hz are widely used in rehabilitation, as they can stimulate sensory and motor nerves for various benefits. Secondly, as the study was conducted exclusively on young adult males, the results may not represent the broader population. Particularly, neuromuscular adaptations are different between men and women. Thus, the minimal differences in such characteristics may have affected the results of this study. Lastly, although the contralateral side was used as the control group, atrophy or neuromuscular changes may also occur in the non-operated limb, potentially overestimating the changes on the contralateral side.

In conclusion, this study demonstrated that the application of NMES following ACLR exerts significant positive effects on neuromuscular function and muscle quality, both of which are commonly impaired after ACLR. However, the results suggest that a three-week NMES intervention may be insufficient to induce optimal improvements in neuromuscular properties, indicating the need for an extended intervention period to achieve more substantial benefits. Furthermore, as individual muscles have different levels of damage in terms of MU behavior and muscle quality, it is suggested that the intervention should be implemented differently depending on the level of damage in individual muscles to achieve efficient results. These findings offer valuable insights into the role of NMES in enhancing neuromuscular function and muscle quality post-ACLR and provide a foundation for designing evidence-based rehabilitation protocols in clinical and athletic training settings.

CONFLICT OF INTEREST

No potential conflict of interest relevant to this article was reported.

ACKNOWLEGMENTS

This study was supported by the Basic Science Research Program through the National Research Foundation of Korea (NRF), funded by the Ministry of Education (NRF-2022S1A5B5A17050057; NRF-2022R1F1A1076564).

REFERENCES

Akima H, Furukawa T. Atrophy of thigh muscles after meniscal lesions and arthroscopic partial menisectomy. Knee Surg Sports Traumatol Arthrosc 2005;13:632-637.

Bezerra P, Zhou S, Crowley Z, Davie A, Baglin R. Effects of electromyostimulation on knee extensors and flexors strength and steadiness in older adults. J Mot Behav 2011;43:413-421.

Davies GJ, McCarty E, Provencher M, Manske RC. ACL return to sport guidelines and criteria. Curr Rev Musculoskelet Med 2017;10:307-314.

Enoka RM, Farina D. Force steadiness: from motor units to voluntary actions. Physiology (Bethesda) 2021;36:114-130.

Farina D, Negro F, Muceli S, Enoka RM. Principles of motor unit physiology evolve with advances in technology. Physiology (Bethesda) 2016;31:83-94.

Hasegawa S, Kobayashi M, Arai R, Tamaki A, Nakamura T, Moritani T. Effect of early implementation of electrical muscle stimulation to prevent muscle atrophy and weakness in patients after anterior cruciate ligament reconstruction. J Electromyogr Kinesiol 2011;21:622-630.

Herda TJ. Resistance exercise training and the motor unit. Eur J Appl Physiol 2022;122:2019-2035.

Herrington L, Ghulam H, Comfort P. Quadriceps strength and functional performance after anterior cruciate ligament reconstruction in professional soccer players at time of return to sport. J Strength Cond Res 2021;35:769-775.

Hollman JH, Nagai T, Bates NA, McPherson AL, Schilaty ND. Diminished neuromuscular system adaptability following anterior cruciate ligament injury: examination of knee muscle force variability and complexity. Clin Biomech (Bristol) 2021;90:105513.

Ikezoe T, Kobayashi T, Nakamura M, Ichihashi N. Effects of low-load, higher-repetition vs. high-load, lower-repetition resistance training not performed to failure on muscle strength, mass, and echo intensity in healthy young men: a time-course study. J Strength Cond Res 2020;34:3439-3445.

Ingersoll CD, Grindstaff TL, Pietrosimone BG, Hart JM. Neuromuscular consequences of anterior cruciate ligament injury. Clin Sports Med 2008;27:383-404, vii.

Jenkins NDM, Rogers EM, Banks NF, Muddle TWD, Colquhoun RJ. Increases in motor unit action potential amplitudes are related to muscle hypertrophy following eight weeks of high-intensity exercise training in females. Eur J Sport Sci 2021;21:1403-1413.

Jo HD, Kim MK. Identification of EIMD level differences between long- and short head of biceps brachii using echo intensity and GLCM texture features. Res Q Exerc Sport 2024;95:441-449.

Jo HD, Kim MK. Involvement of EMG variables and muscle characteristics in force steadiness by level. J Biomed Eng Res 2023;44:336-345.

Johnson MD, Heckman CJ. Gain control mechanisms in spinal motoneurons. Front Neural Circuits 2014;8:81.

Konishi Y, Fukubayashi T, Takeshita D. Mechanism of quadriceps femoris muscle weakness in patients with anterior cruciate ligament reconstruction. Scand J Med Sci Sports 2002;12:371-375.

Koyama Y, Kobayashi H, Suzuki S, Enoka RM. Enhancing the weight training experience: a comparison of limb kinematics and EMG activity on three machines. Eur J Appl Physiol 2010;109:789-801.

Krogsgaard MR, Fischer-Rasmussen T, Dyhre-Poulsen P. Absence of sensory function in the reconstructed anterior cruciate ligament. J Electromyogr Kinesiol 2011;21:82-86.

Kuchinad RA, Ivanova TD, Garland SJ. Modulation of motor unit discharge rate and H-reflex amplitude during submaximal fatigue of the human soleus muscle. Exp Brain Res 2004;158:345-355.

Kyritsis P, Bahr R, Landreau P, Miladi R, Witvrouw E. Likelihood of ACL graft rupture: not meeting six clinical discharge criteria before return to sport is associated with a four times greater risk of rupture. Br J Sports Med 2016;50:946-951.

Labanca L, Rocchi JE, Giannini S, Faloni ER, Montanari G, Mariani PP, Macaluso A. Early superimposed NMES training is effective to improve strength and function following ACL reconstruction with hamstring

 https://doi.org/10.12965/jer.2550086.043

graft regardless of tendon regeneration. J Sports Sci Med 2022;21:91-103.

Labanca L, Rocchi JE, Laudani L, Guitaldi R, Virgulti A, Mariani PP, Macaluso A. Neuromuscular electrical stimulation superimposed on movement early after ACL surgery. Med Sci Sports Exerc 2018;50:407-416.

Lepley LK, Davi SM, Burland JP, Lepley AS. Muscle atrophy after ACL injury: implications for clinical practice. Sports Health 2020;12:579-586.

Lepley LK, Wojtys EM, Palmieri-Smith RM. Combination of eccentric exercise and neuromuscular electrical stimulation to improve biomechanical limb symmetry after anterior cruciate ligament reconstruction. Clin Biomech (Bristol) 2015;30:738-747.

Maffiuletti NA. Physiological and methodological considerations for the use of neuromuscular electrical stimulation. Eur J Appl Physiol 2010;110:223-234.

Mall NA, Chalmers PN, Moric M, Tanaka MJ, Cole BJ, Bach BR Jr, Paletta GA Jr. Incidence and trends of anterior cruciate ligament reconstruction in the United States. Am J Sports Med 2014;42:2363-2370.

Marmon AR, Gould JR, Enoka RM. Practicing a functional task improves steadiness with hand muscles in older adults. Med Sci Sports Exerc 2011;43:1531-1537.

Matta TTD, Pereira WCA, Radaelli R, Pinto RS, Oliveira LF. Texture analysis of ultrasound images is a sensitive method to follow-up muscle damage induced by eccentric exercise. Clin Physiol Funct Imaging 2018;38:477-482.

Mettler JA, Griffin L. Muscular endurance training and motor unit firing patterns during fatigue. Exp Brain Res 2016;234:267-276.

Nishikawa Y, Watanabe K, Takahashi T, Maeda N, Maruyama H, Kimura H. The effect of electrical muscle stimulation on quadriceps muscle strength and activation patterns in healthy young adults. Eur J Sport Sci 2021;21:1414-1422.

Palmieri-Smith RM, Lepley LK. Quadriceps Strength Asymmetry after anterior cruciate ligament reconstruction alters knee joint biomechanics and functional performance at time of return to activity. Am J Sports Med 2015;43:1662-1669.

Palmieri-Smith RM, Thomas AC, Wojtys EM. Maximizing quadriceps strength after ACL reconstruction. Clin Sports Med 2008;27:405-424, vii-ix.

Petrovic I, Amiridis IG, Holobar A, Trypidakis G, Kellis E, Enoka RM. Leg dominance does not influence maximal force, force steadiness, or motor unit discharge characteristics. Med Sci Sports Exerc 2022;54:1278-1287.

Pillen S, Tak RO, Zwarts MJ, Lammens MM, Verrijp KN, Arts IM, van der Laak JA, Hoogerbrugge PM, van Engelen BG, Verrips A. Skeletal muscle ultrasound: correlation between fibrous tissue and echo intensity. Ultrasound Med Biol 2009;35:443-446.

Rice DA, McNair PJ. Quadriceps arthrogenic muscle inhibition: neural mechanisms and treatment perspectives. Semin Arthritis Rheum 2010;40:250-266.

Sahinis C, Kellis E. Hamstring muscle quality properties using texture analysis of ultrasound images. Ultrasound Med Biol 2023;49:431-440.

Skurvydas A, Brazaitis M, Kamandulis S. Repeated bout effect is not correlated with intraindividual variability during muscle-damaging exercise. J Strength Cond Res 2011;25:1004-1009.

Spencer A, Davis K, Jacobs C, Johnson D, Ireland ML, Noehren B. Decreased quadriceps force steadiness following anterior cruciate ligament reconstruction is associated with altered running kinematics. Clin Biomech (Bristol) 2020;72:58-62.

Wellauer V, Item JF, Bizzini M, Maffiuletti NA. Home-based nonoperative-side quadriceps neuromuscular electrical stimulation prevents muscle weakness following anterior cruciate ligament reconstruction. J Clin Med 2022;11:466.

Yang JH, Eun SP, Park DH, Kwak HB, Chang E. The effects of anterior cruciate ligament reconstruction on individual quadriceps muscle thickness and circulating biomarkers. Int J Environ Res Public Health 2019;16:4895.

Zaheer F, Roy SH, De Luca CJ. Preferred sensor sites for surface EMG signal decomposition. Physiol Meas 2012;33:195-206.